



# Calculation of Linear Damping Coefficients by Numerical Simulation of Steady State Experiments

A. Shadlaghani<sup>1</sup> and S. Mansoorzadeh<sup>2†</sup>

<sup>1</sup> Department of Mechanical Engineering, Isfahan University of Technology, Isfahan, 8415683111, Iran

<sup>2</sup> Research Institute for Subsea Science & Technology, Isfahan, 8415683111, Iran

†Corresponding Author Email: [Shahriar@cc.iut.ac.ir](mailto:Shahriar@cc.iut.ac.ir)

(Received December 14, 2014; accepted April 29, 2015)

## ABSTRACT

The aim of the present study is to investigate the superiority of steady tests simulations relative to the unsteady experiments, especially planar motion mechanism tests (PMM), for computing velocity-based hydrodynamics coefficients. Using CFD analysis, steady maneuvers including towing with drift and attack angles together with rotating arm tests are simulated in order to calculate the linear damping coefficients of a prototype submarine. Comparisons of the obtained results with available unsteady experimental results of the SUBOFF submarine show the reliability of the methods used in this paper. It also demonstrates the accuracy and simplicity of the present simulations due to the steady nature of simulations. In order to compute the linear damping coefficients, the simulations have been performed in small values of the attack and drift angles and angular velocities for the towing and rotating arm tests, respectively.

**Keywords:** Damping coefficient; Numerical simulation; Drift and attack angles; Rotating arm.

## NOMENCLATURE

$C_f$	skin drag coefficient	$X_{prop}$	X component of the thrust force
$C_p$	pressure coefficient	$x$	component of added mass coefficient
$f_i$	body force	$Y_y$	y component of added mass coefficient
$i, j$	displacement directions index	$Z_w$	z component of added mass coefficient
$K, M, N$	x, y, z components of Moments	$\alpha$	angle of attack
$P$	pressure	$\beta$	angle of drift
$p, q, r$	angular velocities	$\rho$	density
$u, v, w$	linear velocities	$\nu$	kinematic viscosity
$u'_i$	fluctuating velocity		

## 1. INTRODUCTION

Underwater vehicles have been become inevitable tools in underwater operations, oil industries, oceanography, and military purposes. In order to explain the dynamic behavior of these vehicles, the governing equations of motion should be solved. Dynamic performance of underwater vehicles directly relates to the external forces including hydrostatic, hydrodynamic, propeller, and reflective forces due to the control surfaces angle. These forces depend on many parameters such as vehicle shape, propulsion, buoyancy, etc. Hydrodynamic forces and moments are usually described in terms of hydrodynamic coefficients in the motion equations. Added mass and damping coefficients are the two main categories of the hydrodynamic coefficients. Identifying the hydrodynamic

coefficients is necessary to analyze the six degrees of freedom motions. Several methods such as analytical, semi-empirical, experimental, and computational approaches can be used for evaluating the hydrodynamic coefficients. Analytical methods are chiefly used to determine the hydrodynamic coefficients of simple geometries. Using the semi-empirical approaches is limited to derive the approximate formulas from the experimental data. Experimental studies are the conventional means for obtaining the hydrodynamic coefficients that involve the towing tests, rotating arm, planar mechanism motions (PMM), etc. Computational fluid dynamic (CFD) is another method to acquire the hydrodynamic derivatives by simulating the experimental maneuvers. Numerical methods solve the Navier-Stokes equations numerically and are compatible with complicated

geometries. Phillips *et al.* (2007) simulated the pure sway motion numerically to determine the hydrodynamic coefficients of an Autonomous Underwater Vehicle (AUV). He also showed that the coefficients derived from unsteady simulations have a slight dependence on the time step sizes. Bellevre *et al.* (2000) analyzed the submersibles motions using the numerical method with Reynolds Averaged Navier-Stokes equations (RANS) simulation. Zhang *et al.* (2010) calculated the hydrodynamic coefficients of an AUV by simulating the PMM maneuver and turning motions. He also established a simulation system, consisting of force module, inertial coefficient module and acceleration module to predict the maneuverability of AUV during the scheme design stage with usage of the obtained coefficients. Yucun *et al.* (2012) also computed the damping coefficients of a submarine with simulating the PMM and oblique tests and compared the obtained results with those of the experimental tests. Tang *et al.* (2009) calculated the damping and inertial coefficients of an AUV with complex geometry using CFD method. Hu *et al.* (2008) proposed added momentum sources-based method to compute hydrodynamic coefficients of an underwater vehicle, and compared their results with the results obtained from scaled model tests. Baker (2004) estimated the drag force of a submarine using a commercial code by simulating the steady tests, and compared his results with the wind tunnel experiments. Ayub *et al.* (2005) investigated the effects of geometrical parameters such as length and diameter on the hydrodynamic forces of a submarine in steady motions. Brogolia *et al.* (2007) simulated the horizontal PMM motion for a submersible model using CFD code with considering the free surface effects, and compared his results with experimental data.

It is almost accepted that PMM simulations are the prevalent procedure for calculating the hydrodynamic derivatives and consequently damping coefficients. However, the unsteady nature of the PMM tests simulations and using the moving mesh technique for representing the motions boost the time and cost of the calculations. Nair *et al.* (2010) simulated an unsteady high speed flow over a blunt body and demonstrated that time step can influence on the stability of numerical method generally. In addition, amplitude and frequency of oscillations have considerable effects on the obtained results. Ryan Coe (2012) investigated these effective parameters on the PMM simulations results. In this paper, for avoiding the mentioned problems of PMM simulations, linear damping coefficients of a submarine are computed by simulating the steady state tests. These maneuvers include the towing of the model, with various attack and drift angles, and rotation of the model in the different angular velocities.

## 2. MOTION EQUATIONS AND MODEL

In order to explain the motions of submerged body,

two coordinate systems should be defined. One is the inertial frame and the other is the body fixed-frame, which its origin is located at the center of buoyancy or gravity. These two coordinate systems and the symbols used for the definition of forces and moments are shown in Fig. 1.  $[u \ v \ w \ p \ q \ r]$  are the linear and angular velocities and  $[X \ Y \ Z \ K \ M \ N]$  are the forces and moments, acting on the model.

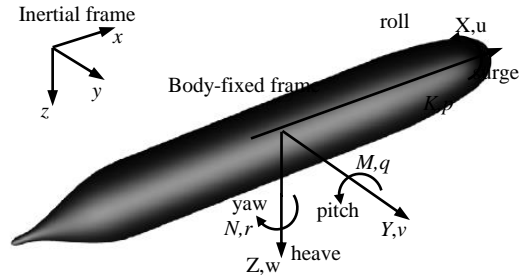


Fig. 1. Definition of coordinate systems.

The planar maneuvering simplifies the motion equations to a set of linear equations. Using the hydrodynamic derivative notation,  $Y_v = \partial Y / \partial v$ ,  $Y_r = \partial Y / \partial r$ , etc., the linearized equations of motion in the horizontal plane are defined as follows:

$$\begin{aligned}
 \text{Surge} : (m - X_{\dot{u}})\dot{u} &= X_u(u + U) + X_{prop} \\
 \text{Sway} : (m - Y_{\dot{v}})\dot{v} + (mx_G - Y_{\dot{r}})\dot{r} &= Y_v v \\
 &+ (Y_r - mU)r + Y_{\delta}\delta \\
 \text{Yaw} : (mx_G - N_{\dot{r}})\dot{v} + (I_z - N_{\dot{r}})\dot{r} &= N_v v \\
 &- (N_r - mx_G U)r + N_{\delta}\delta
 \end{aligned} \tag{1}$$

Also in the vertical plane, linearized equations are defined as follows:

$$\begin{aligned}
 \text{Surge} : (m - X_{\dot{u}})\dot{u} &= X_u u + X_q q - X_{\theta}\theta \\
 \text{Heave} : (m - Z_{\dot{w}})\dot{w} - (mx_G + Z_{\dot{q}})\dot{q} &= Z_w w \\
 &+ (Z_q + mU)q + Z_{\delta}\delta \\
 \text{Pitch} : -(mx_G + M_{\dot{w}})\dot{w} + (I_y - M_{\dot{q}})\dot{q} &= M_w w \\
 &+ (M_q - mx_G U)q + M_{\theta}\theta + M_{\delta}\delta
 \end{aligned} \tag{2}$$

In the above equations,  $m$  and  $C_G = [x_G, y_G, z_G]$  are the mass and gravity center of vehicle.  $\delta$  and  $U$  are the control surface angle and towing velocity of the vehicle respectively.  $I_z$  and  $I_y$  are the inertial moments and  $\theta$  is the pitch angle.

In this study, the DARPA SUBOFF submarine has been chosen for simulations because its hydrodynamic coefficients are available and can be used to validate the numerical results. This submarine was designed in the David Taylor Research center (DTRC), and a series of experiments have been carried out to measure its experimental and hydrodynamic data by Roddy (1990). Its geometrical properties are represented in table 1.

**Table 1 Geometrical properties of SUBOFF submarine**

Description	Magnitude	Unit
Total length	4.356	m
maximum diameter	0.508	m
Volume of displacement	0.718	m <sup>3</sup>
Wetted surface	6.33	m <sup>2</sup>

Figure 2 shows the sketch of the submarine including bare hull, sail and control surfaces.



**Fig. 2. Sketch of DARPA SUBOFF geometry.**

### 3. SOLUTION PROCEDURE

In this section, the procedure of determining the hydrodynamic forces and moments, and also formulating them in terms of the damping coefficients are discussed. Here, in order to compute the damping coefficients, the steady hydrodynamic experiments are explained. By towing the model with attack and drift angle, and rotating the model in the rotating arm facilities, the corresponding coefficients to the linear and angular velocity are computed respectively.

#### 3.1 Towing Test

When a submerged body is towed with a constant speed of  $U$  at a specific drift angle of  $\beta$ , the model has both surge and sway velocity components. These velocities are functions of  $\beta$  as shown in the Fig. 3.

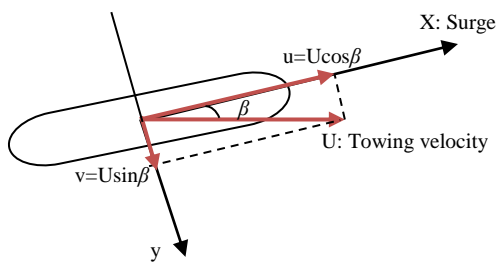


**Fig. 3. Towing experiment with drift angle.**

Therefore, in addition to the axial force, the sway force and yaw moment act on the model. If this experiment is repeated for different small values of drift angle  $\beta$ , the variation of  $Y$  and  $N$  versus sway velocity component can be plotted. Referring to the definition of the hydrodynamic derivatives:

$$Y_v = \frac{\partial Y}{\partial v} = \frac{\partial Y}{\partial (U \sin \beta)} = \frac{1}{U} \frac{\partial Y}{\partial \beta} \quad (3)$$

$$N_v = \frac{\partial N}{\partial v} = \frac{\partial N}{\partial (U \sin \beta)} = \frac{1}{U} \frac{\partial N}{\partial \beta}$$

Therefore, the slope of the plotted curve at the origin represents the damping coefficients  $Y_v$  and  $N_v$ . By replicating this experiment for small attack angles  $\alpha$  in the vertical plane, variation of  $Z$  and  $M$  versus heave velocity component can be used to obtain  $Z_w$  and  $M_w$ , defined in Eq. (4). In order to obtain the coefficients using the above equations, the range of angles should be small. The angles between 0 to 12 degrees are considered for all towing simulations.

$$Z_w = \frac{\partial Z}{\partial w} = \frac{\partial Z}{\partial (U \alpha)} = \frac{1}{U} \frac{\partial Z}{\partial \alpha} \quad (4)$$

$$M_w = \frac{\partial M}{\partial w} = \frac{\partial M}{\partial (U \alpha)} = \frac{1}{U} \frac{\partial M}{\partial \alpha}$$

#### 3.2 Rotating Arm Test

In the rotating arm test, the model is linked to an arm that rotates in a horizontal plane about a fixed axis at the center of the tank.

The longitudinal axis of model should always be normal to the arm at the center of gravity or buoyancy. The surge velocity should be constant and equals to  $u=l.r$ , and sway velocity  $v$  always remains zero (Fig. 4), where,  $l$  and  $r$  are the length and angular velocity of the rotating arm, respectively. To have a constant surge velocity, as the angular velocity changes, the length of the arm should be changed accordingly. By plotting the computed sway force  $Y$  and the yaw moment  $N$  versus various angular velocities  $r$ , the damping coefficients  $Y_r$  and  $N_r$  can be calculated.

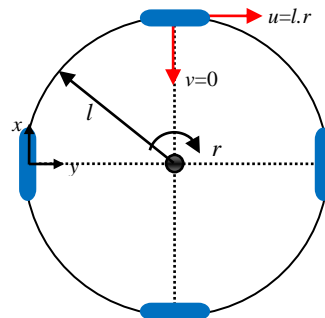


**Fig. 4. Rotating arm experiment.**

Here again, the slopes at the origin correspond to the linear coefficients, therefore, angular velocities should be small.

### 4. NUMERICAL ANALYSIS

Appearance of eddy motions in turbulent flows causes exact solution of NS equations to be expensive. The motion of the fluid is modeled using the RANS equations in order to determine the flow

variables. These equations for incompressible and isothermal flow can be expressed as Eq. (5)

$$\frac{\partial u_i}{\partial x_i} = 0$$

$$\frac{\partial u_i}{\partial t} + \frac{\partial u_i u_j}{\partial x_j} = -\frac{\partial P}{\partial x_i} + \nu \frac{\partial}{\partial x_j} \left( \frac{\partial u_i}{\partial x_j} + \frac{\partial u_j}{\partial x_i} \right) - \frac{\partial u'_i u'_j}{\partial x_j} + f_i \quad (5)$$

Fluctuations associated with turbulence add an extra Reynolds stress as  $(u'_i u'_j)$  on the mean flow. In particular, it is required to relate the Reynolds stress to the known flow variables. Turbulence models are a computational procedure to close the momentum equations in order to the variety of flow field can be calculated. In this study, SST turbulence model is used in all simulations because of its robustness for introducing the separation point.

The finite volume method is used to discretize the NS equations using the high-resolution scheme for modeling the advection and turbulence terms. The residual target of conservation and momentum equations is set at  $10^{-5}$  for all simulations to achieve the convergence.

#### 4.1 Fluid Domain and Boundary Conditions

A cubic domain is considered for towing tests simulations. The used boundary conditions are shown in Fig. 5.



Fig. 5. Boundary conditions for towing test.

The boundary conditions on the domain consist of:

- Velocity inlet, which is located one-body lengths upstream, with a magnitude of 2m/s.
- Outlet, which is located three-body lengths upstream, with zero static pressure condition.
- Outer domain, which is located eight-diameters away from the model with free slip wall condition.
- The submarine surface which is modeled with the non-slip wall condition.

As shown in Fig. 6, a segment of circle with a rectangular cross section is established for the rotating arm domain. The dimensions and boundary conditions are similar to the towing domain with a few extra conditions.

In this case, the domain is defined as a rotating domain with its origin at the center of rotation. Also, at the inlet, velocity is linearly changed along the arm (here along the y-axis) to give a velocity of 2m/s for submarine at the centerline of the model.

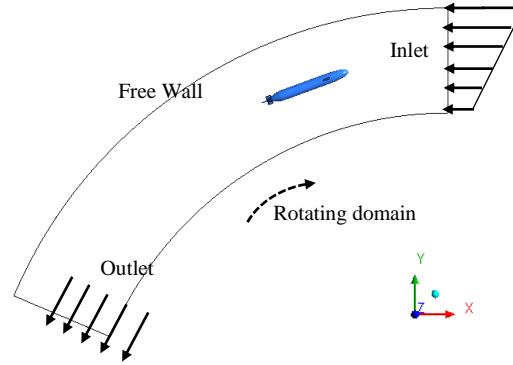


Fig. 6. Boundary conditions for rotating arm test.

#### 4.2 Grid Definition

The unstructured grids are used for generating elements on the model surface and fluid domain. In order to increase the accuracy of solution inside the boundary layer, density of grids is increased near the surface of the model. In the boundary layer zone, prism elements are generated to increase the number of elements in the normal direction of the surface. Therefore, exact estimation of the first layer thickness and number of layers is essential in the boundary layer. The thickness of boundary layer and the first layer for a blunt body for a favor  $y^+$  can be estimated from the following equations:

$$\delta = 0.035 L Re^{-1/7} \quad (6)$$

$$\Delta y = L y^+ \sqrt{80} Re^{-13/14} \quad (7)$$

Since the submarine velocity has been considered to be 2m/s in simulations, the thickness of boundary layer  $\delta$  is about 15mm. The first layer thickness is 0.6mm for an expecting  $y^+$  of 40. Therefore, the entire boundary layer is covered using 11 layers with a height ratio of 1.4 from the surface. Note that, when the model is towed with drift or attack angle, the thickness of boundary layer becomes more than the above value. Figure 7 shows the grids used for the simulations.

In the numerical analysis, the sensitivity of the solution to the number and size of grids should be investigated. Since the size of elements depends on the viscous parameter, skin drag coefficient could be an appropriate criterion for choosing the best grids. The obtained results for a series of generated grids are compared to check the results variation. The properties of the used grids are shown in table 2.

Table 2 Properties of grids study

	$\alpha=0^0$	$\alpha=7^0$
	Total elements	Total elements
Coarse	833864	1126200
Medium	1106616	1332427
Fine	1359877	1663503
Fine (1)	1878225	2028558
Fine (2)	2534171	2409184

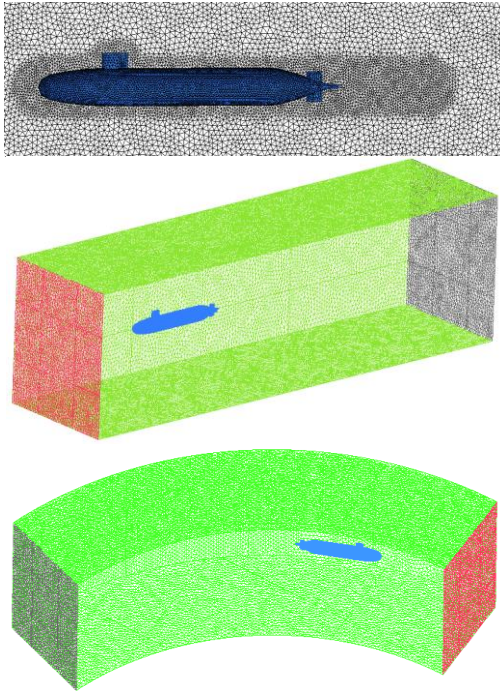


**Fig. 7. Unstructured grids around the submarine.**

The variations of skin drag coefficients according to the table 2 are indicated in Fig. 8 for both  $\alpha=0$  and  $7^\circ$ .

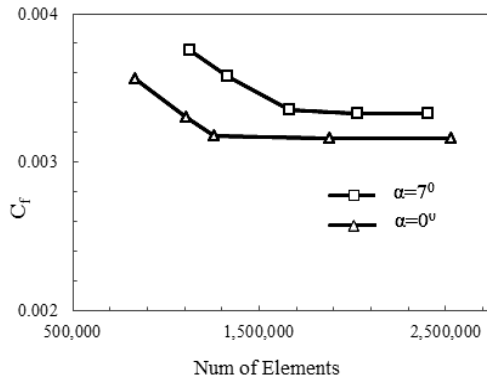


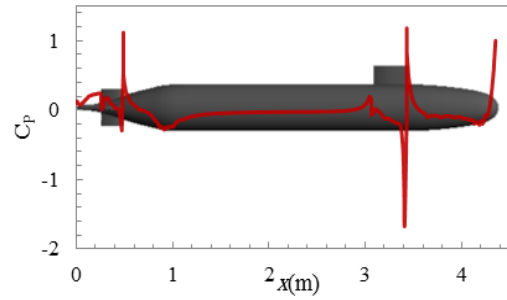
**Fig. 8. Skin drag coefficients variations.**

The difference between the skin drag coefficient obtained from the Fine and Fine (1) grids is negligible; therefore, the Fine grid is finally used to perform the rest of simulations in order to save computational time.  $C_P$  shows the pressure variation for each surface element over the model and introduced as follow:

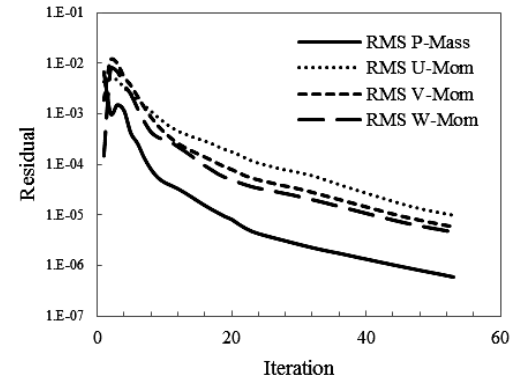
$$C_P = \frac{P - P_\infty}{0.5\rho V^2} \quad (8)$$

Figure 9 indicates the  $C_P$  variation over the submarine at the zero angle of attack.

The convergence of mass and momentum equations for the towing motion at  $\alpha=7^\circ$  is shown in the Fig. 10.



**Fig. 9.  $C_P$  distribution over the  $x$  axis at  $\alpha=0^\circ$ .**



**Fig. 10. Convergence of the results for towing motion at  $\alpha=7^\circ$ .**

## 5. RESULTS AND DISCUSSION

The towing simulations are performed for small angles including 0,1,2,3,5,7,10,12 degrees. Figures 12 to 15 show the variations of the damping forces and moments with the attack and drift angles. It has been illustrated that the slope at the origin represents the coefficients values. As shown in Figs. 12 and 14, the slopes of the obtained curves for the variation of  $Y$  and  $Z$  forces with drift and attack angles, respectively, are negative. This indicates that both  $Y_v$  and  $Z_w$  have negative values. Figure 11 can be used to justify the obtained results.

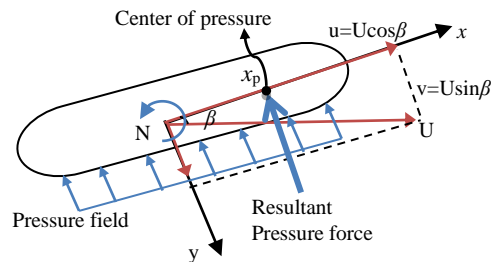


**Fig. 11. Towing the vehicle with a drift angle.**

As shown in this figure, when the vehicle is towed with a positive drift angle of  $\beta$ , a sway velocity of  $U \sin \beta$  in the positive  $y$  direction appears. In this case, as shown in Fig. 11, a pressure field develops near the starboard (right side) of the vehicle. The resultant pressure force (the total sum of the pressure forces) acts on the center of pressure,  $x_p$ , in the negative direction of  $y$  axes. Therefore the sway force  $Y$  and the sway velocity  $v$  are in opposite directions and therefore  $Y_v = \partial Y / \partial v$ , is negative. As

the drift angle increases further, both the sway velocity and sway force increases. This agrees with what can be seen in Fig. 12. Variation of Z force with angle of attack, as shown in Fig. 14 can be interpreted similarly. Comparing Figs. 12 and 14 indicates that, for a specific drift or attack angle, the Y force is significantly larger than the Z force. This is due to the presence of the sail structure, which increases the resistance force, when the vehicle moves with a drift angle of  $\beta$ . Hence, one expect that  $Y_v$  to be larger than  $Z_w$

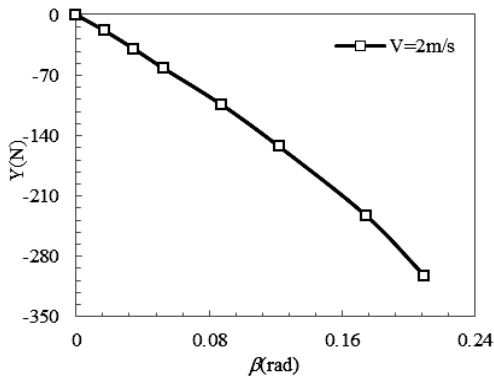


Fig. 12. Variations of sway force with drift angle.

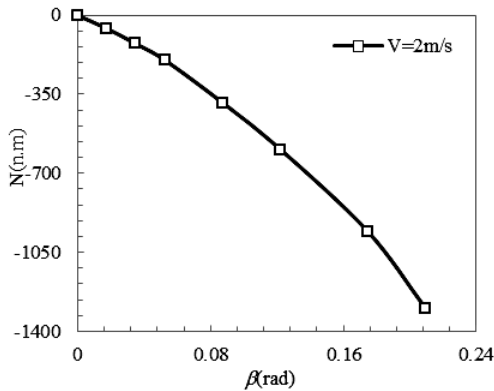


Fig. 13. Variations of yaw moment with drift angle.

The direction or sign of N depends on the direction of the resultant pressure force and the location of center of pressure. As shown in Fig. 11, the direction of the resultant pressure force is in the negative y direction. If the center of pressure  $x_p$  is located in the positive direction, the N moment has a negative sign (counter clock wise direction), but if  $x_p$  is located in the negative direction, the N moment has a positive sign (clock wise direction). Figure 13 shows that N has a negative value. Therefore the center of pressure in the SUBOFF submarine is located in the front of the origin (center of mass). Since the N moment and v velocity are in the opposite directions,  $N_v$  is a negative number. Similar reasoning can be stated for the obtained results shown in Fig. 15.

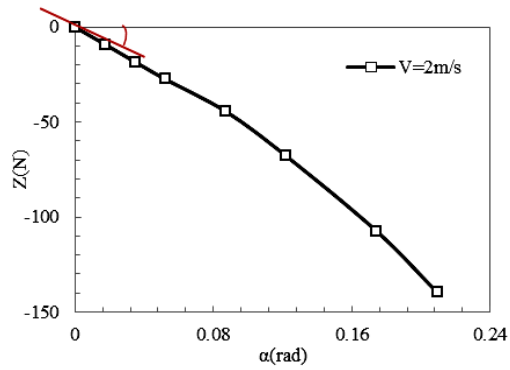


Fig. 14. Variations of heave force with attack angle.

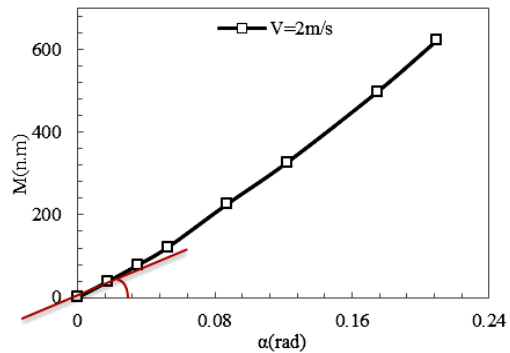


Fig. 15. Variations of pitch moment with attack angle.

The rotating arm simulations are also performed for small angular velocities including 0.05, 0.06, 0.07, 0.08, 0.09, 0.1, 0.11 rad/s. Figures 15 and 16 show the variations of the sway force and yaw moment with the angular velocities.

In these cases, because of the irregular variations of the force and moment with angular velocities, slopes of the linear average at origin are considered as the coefficients values.

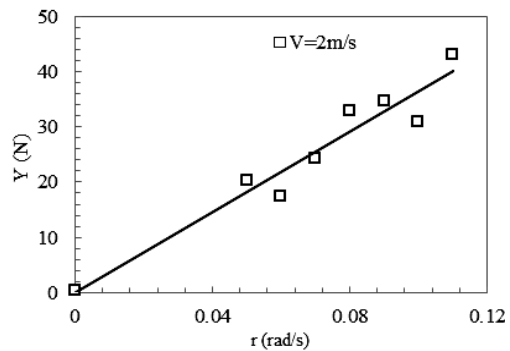
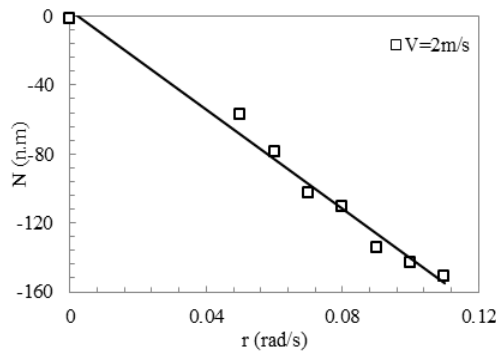


Fig. 16. Variations of sway force with angular velocity.

It should be noted that since the pressure gradient is negative, the sway force Y is in the positive y direction. In addition, since the sway force increases with angular velocity,  $Y_r$  is positive. This agrees with what was observed in Fig. 16. Variation

of Yaw moment  $N$ , with angular velocity, shown in Fig. 17, indicates that as the angular velocity increases the negative value of  $N$  also increases, indicating a negative value for  $N_r$ .



**Fig. 17. Variations of yaw moment with angular velocity.**

As it was explained earlier, the planar motion mechanism test is another way to calculate linear damping coefficients. For representing the PMM maneuvers, the sinusoidal motion should be simulated using moving mesh techniques.

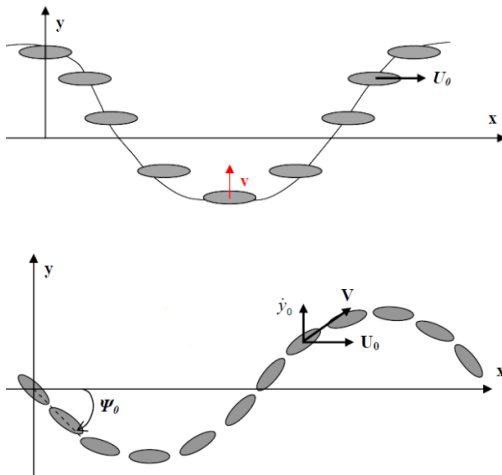


**Fig. 18. PMM motions (sway oscillation and fish experiment).**

In the PMM simulations, the fluid domain is split into moving inner and fixed outer regions, which inner domain moves laterally within the outer domain. Yu-cun (2012) simulated these motions (Fig. 18) numerically and monitored the acted forces and moments to compute the hydrodynamic derivatives.

The computed coefficients are non-dimensionalised using the length of the vehicle ( $L$ ), the velocity ( $V$ ) and the angular velocity ( $r$ ) of the vehicle, and the density of the fluid ( $\rho$ ).

$$Y' = \frac{Y}{0.5\rho u^2 L^2}, \quad N' = \frac{N}{0.5\rho u^2 L^3} \quad (9)$$

$$r' = \frac{rL}{u}, \quad v' = \frac{v}{U}$$

Similar procedure is used to non-dimensionalise the heave force ( $Z$ ) and pitch moment ( $M$ ). The obtained coefficients from both methods are compared with the experimental results (1990), which are shown in table 4.

**Table 4 Comparison of damping coefficients**

	Present work	PMM results (2012)	Exp. Reports (1990)
$Y'_v$	-0.0281	-0.0303	-0.0278
$N'_v$	-0.014	-0.0131	-0.0136
$Z'_w$	-0.015	-0.0157	-0.0139
$M'_w$	0.011	0.0103	0.0103
$Y'_r$	0.0044	0.0046	0.0052
$N'_r$	-0.004	-0.0042	-0.0044

According to table 4, the results obtained from the steady state simulations are very close to those obtained by PMM tests. However, simulation of steady experiments is much simpler than that of PMM.

The fluid velocity distribution around the model for the towing and rotating motion at the specified angle and arm length is shown in Figs. 19 and 20.

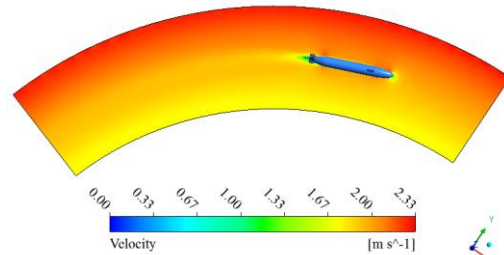


**Fig. 19. Velocity contour at  $r=0.11$ rad/s around the model.**

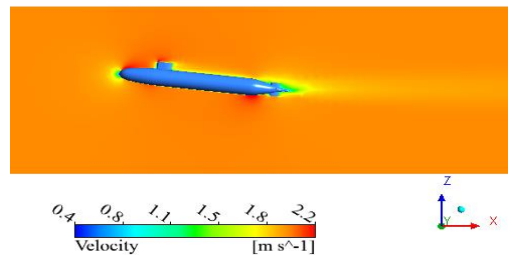


**Fig. 20. Velocity contour at  $\alpha=7^\circ$  around the model.**

## 6. CONCLUSION

In this paper, steady state maneuvers of a submarine including towing with angle of drift/attack and rotating arm were numerically simulated to calculate six linear damping coefficients including the translational and rotational coefficients. Comparing the present method with the conventional method, which uses planer motion mechanism (PMM), to calculate the hydrodynamics coefficients, indicates that the present method is both simpler and more cost effective. Simulations of the PMM maneuvers are numerically

complicated and expensive. In addition, the obtained results are functions of amplitude and frequency of oscillations. The unsteady simulation results are also a function of the time steps used in the numerical simulations. In this paper it was shown that the expensive and complicated unsteady simulations of PMM maneuvers can be replaced by simple steady state simulations of towing and rotating of the model. The resulting velocity dependent (translational) hydrodynamic coefficients obtained from the present steady simulations, at small angles of drift or attack, were shown to be comparable with the corresponding reported numerical and experimental results. The rotational hydrodynamics coefficients obtained from rotating arm simulations also agreed well with the corresponding results obtained from the PMM experimental and numerical simulations. The present method can also be used to estimate the direction and center of action of the pressure forces and moments of a submarine.

#### REFERENCES

- Ayub, A. M., M. Sohaib, S. Bilal, S. Zahir, M. A. Khan (2005). *Estimation of Hydrodynamic Coefficient of DARPA-2 and Their Geometry Dependence*. National Engineering and Scientific Commission Magazine, Islamabad 43.
- Baker, C. (2004). *Estimating Drag Forces on Submarine Hulls*. Senior report, University of New Brunswick, Canada, January.
- Belleve, D., de. Diaz, A. Tuesta and P. Perdon (2001). Submarine Manoeuvrability assessment using Computational Fluid Dynamic Tools, *Proc. 23rd Symposium of Naval Hydrodynamics*, Val de Reuil, France, pp. 820-832.
- Brogolia, R., A. D. Mascio and G. A. Amati (2007). Parallel unsteady RANS code for the numerical simulations of free surface flows. *2nd international Conference on Marine Research and Transportation*, Ischia (NA), Italy, June.
- Coe, R. and W. Neu (2012). Amplitude effects on virtual PMM tests. *Conference of oceans 1-5*
- Hu, Z. and Y. Lin (2008). Computing the Hydrodynamic Coefficients of Underwater Vehicles Based Added Momentum Sources. *International Offshore and Polar Engineering Conference*, Vancouver, BC, Canada, July.
- Nair. P., T. Jayachandran, M. Deepu, B. P Puranik and U. V. Bhandarkar (2010). Numerical Simulation of Interaction of Sonic Jet with High Speed Flow over a Blunt Body using Solution Mapped Higher Order Accurate AUSM UP Based Flow Solver. *Journal of Applied Fluid Mechanics* 3(1), 15-23.
- Phillips, A., M. Furlong and S. R. Turnock (2007). "Virtual planar motion mechanism tests of the autonomous underwater vehicle autosub. *STG-Conference/Lectureday CFD in Ship Design*, Hamburg, Germany.
- Roddy, R. F. (1990). *Investigation of the stability AMD control characteristic of several configuration of the darppa suboff model from captive-model experiment*. DTRC/SHD, 1-108.
- Tang, S., U. Tamaki, N. Takeshi, B. Thornton and T. Jiang (2009). Estimation of the hydrodynamic coefficients of the complex-shaped autonomous underwater vehicle TUNA-SAND. *Journal of Marine Science and Technology*. 14(3), 373-386.
- Yu-cun, P., Z. Huai-xin and Z. Qi-dou (2012). Numerical prediction of submarine hydrodynamic coefficient using CFD simulation. *Journal of hydrodynamic* 24(6), 840-847.
- Zhang, H., Xu, Yu-ru., Cai., Hao-peng. (2010). Using CFD Software to Calculate Hydrodynamic Coefficient. *Journal of Marine Science and Application* 9(2), 149-155.